JOURNAL OF CATALYSIS 151, 147–154 (1995)

A Comparative Study of the Microporosity of the Ammonium and Cesium Salts of 12-Tungstophosphoric, 12-Molybdophosphoric, and 12-Tungstosilicic Acids by Xe^{129} NMR

J. L. Bonardet,* J. Fraissard,* G. B. McGarvey,† and J. B. Moffat†,[1]

*Laboratoire de Chimie des Surfaces, Université Pierre et Marie Curie, Paris, France; and †Department of Chemistry and the Guelph–Waterloo Centre for Graduate Work in Chemistry, University of Waterloo, Waterloo, Ontario, Canada N2L 3G1

Received February 28, 1994; revised August 18, 1994

The Xe^{129} NMR method has been applied to the ammonium and cesium salts of 12-tungstophosphoric, 12-molybdophosphoric, and 12-tungstosilicic acids, as well as to the potassium salt of the first acid. The data obtained provide evidence for the presence of a homogeneous and organized pore structure. The ammonium salts produce similar pore openings of 9.0 Å, regardless of the composition of the anion, while those for the cesium salts are found to be dependent on the nature of the anion. © 1995 Academic Press, Inc.

INTRODUCTION

The synthesis of porous solids is of continuing interest in catalysis (1). While small pore catalysts such as the ZSM family of zeolites, and particularly ZSM-5, have been and continue to be of importance in shape-selective processes (2), increasing emphasis is being placed on larger pore materials (3).

Although the existence of pores is, with some solids, a consequence of the crystallographic structure, with others the synthetic procedures may be of prime importance. Thus certain elemental compositions, such as those containing aluminum, silicon, and oxygen together with one or more cations, may, on one hand, have little or no porosity, while, on the other hand, may contain pores of reproducible geometry. The use of organic structure-directing agents in the preparation of porous zeolitic structures has now become an established technique (4), while the adjustment of pore sizes by cation exchange in zeolites such as faujasites is already well known (5).

Work in one of our laboratories has been concerned, among other things, with metal–oxygen cluster compounds (MOCC) (also known as heteropoly oxometalates). Although these appear in a variety of forms, perhaps the most common are those whose anions have Keggin structure (Fig. 1) (6). A central atom such as phosphorus is surrounded by four oxygen atoms arranged tetrahedrally. Twelve octahedra with oxygen atoms at their vertices and a peripheral metal atom such as tungsten at their approximate centers envelope the central tetrahedron and share oxygen atoms with each other and the tetrahedron.

The MOCC, regardless of the composition of the anions, have discrete ionic structures unlike the network structure found with many zeolites. The MOCC with phosphorus at the center of the anions, tungsten in the peripheral metal positions, and protons as the cations, 12-tungstophosphoric acid ($H_3PW_{12}O_{40}\cdot nH_2O$), has cubic *Pn3m* crystallographic structure (7) (Fig. 2). Although all of the MOCC with protons as cations have not been measured, those which have show small surface areas (less than 10 $m^2\ g^{-1}$).

Work in this laboratory has shown, in part, from the analysis of nitrogen adsorption–desorption isotherms, that certain of the salts of the MOCC prepared with monovalent cations have relatively high surface areas and porous structures (8–30). Thus, for example, the surface area of the ammonium salt of 12-molybdophosphoric acid is approximately 190 $m^2\ g^{-1}$ and the average pore radius is 13 Å, while that of the sodium salt is only 4 $m^2\ g^{-1}$ (8, 9, 23). The pore structures are evidently not only dependent on the nature of the cation but also on the elemental composition of the anion (10, 11, 15, 23). For example, the surface areas of 12-tungstosilicic and 12-tungstophosphoric acids are measured as 117 and 128 $m^2\ g^{-1}$ (8–11). However, recent studies have shown that the surface areas and pore structures are dependent upon the relative amounts of the preparative reagents, as well as the temperatures to which the resulting solid is exposed (28, 29). Studies of the alkylation of toluene with methanol as well as substituent-group rearrangements of methylethylbenzenes have provided indirect evidence for the presence of the porous structures (21, 22). Measurements of the sorption and diffusion of alkanes, alkenes, aromatics, and alcohols have also provided evidence for

[1] To whom correspondence should be addressed.

0021-9517/95 $6.00

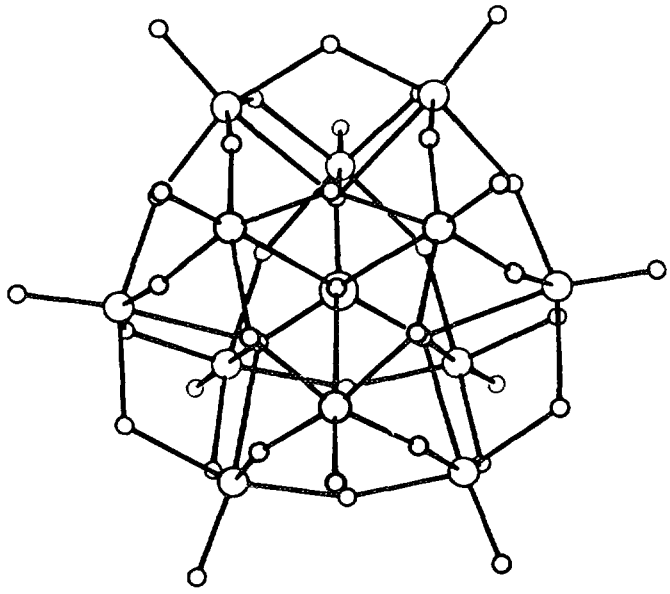

FIG. 1. Anion of Keggin structure (bigger circles, central and peripheral atoms; smaller circles, oxygen atoms).

the existence of the porous structures (12, 17–20, 25). More recent work has shown that the cations of the high surface area salts of 12-tungstophosphoric and 12-molybdophosphoric acids can be exchanged, at least partially, with semiquantitative retention of the pore structures (26, 27). A preliminary account of Xe^{129} studies has been reported (31).

Information on the nature and source of the microporous structure of the monovalent salts of the MOCC can be obtained from nitrogen adsorption–desorption isotherms and from X-ray diffraction analysis (23). With the microporous salts, the intensity of the [110] reflection relative to that of the [222] plane, the latter of which is usually the most intense reflection, shows an approximately inverse relationship to the micropore volume, regardless of the anion composition. From a hard-sphere ion-packing model, it is apparent that the solids contain interstitial voids separated from each other by the terminal oxygen atoms of the anions and capable of alignment with each other in directions parallel to or normal to the [110] plane of the crystal. As the size of the cation increases, the cubic lattice parameter also increases, and the anions will translate and rotate with consequent widening of the interstitial voids. Thus the terminal oxygen atoms of the anions may move from their original positions, leading to a reduction of the [110] intensity, the formation of connections between the interstitial voids, and the creation of channels lying parallel to and normal to this plane.

The aforementioned surface area and pore size distribution data were obtained by appropriate analyses of nitrogen adsorption isotherms. The application of a method which would provide independent confirmation of the results calculated from the adsorption data appeared to be both appropriate and desirable. The Xe^{129} NMR method developed by Fraissard and Ito [see (32, 33)] has been applied to a wide variety of solids ranging from zeolites to polymers, with considerable success (34). In the present work, this technique is applied to the ammonium and cesium salts of 12-tungstophosphoric ($H_3PW_{12}O_{40}$, abbreviated HPW), 12-molybdophosphoric ($H_3PMo_{12}O_{40}$, abbreviated HPMo), and 12-tungstosilicic ($H_4SiW_{12}O_{40}$, abbreviated HSiW) acids, as well as to the potassium salt of the first acid. These choices permit the examination of both the effect of the composition of the anion and the nature of the cation.

EXPERIMENTAL

The ammonium and cesium salts of HPW, HPMo, and HSiW and the potassium salt of HPW were prepared as described earlier (8, 10).

The samples were preheated at 473 K under vacuum ($P < 10^{-2}$ Pa) for 12 h prior to the adsorption measurements. Xenon isotherms were obtained on a classical volumetric apparatus at 300 K and *in situ* at 223 and 273 K.

NMR spectra were obtained with the classical $\pi/2$ sequence impulsion and were recorded with a CXP-100 Bruker apparatus at 24.9 MHz. The time delay was 0.5 s. Between 5000 and 200,000 scans were taken. The esti-

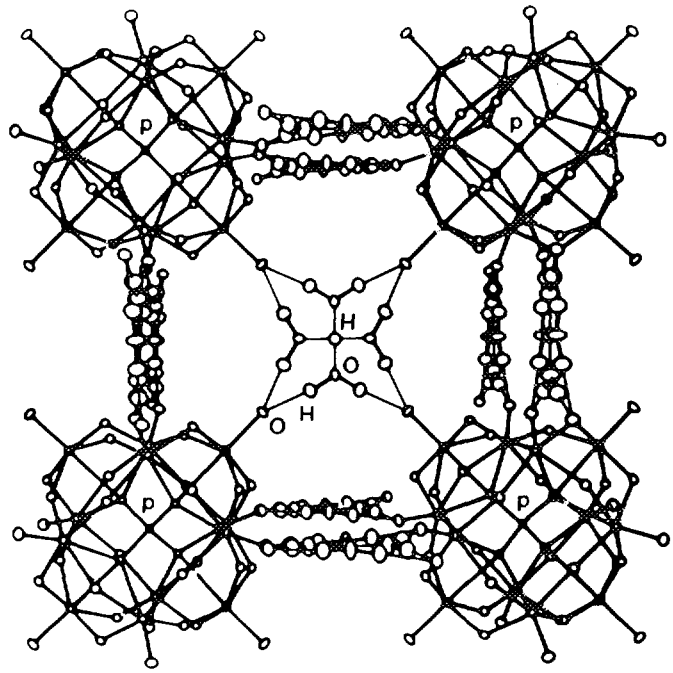

FIG. 2. Structural arrangement of anions, protons, and water molecules in 12-tungstophosphoric acid (7).

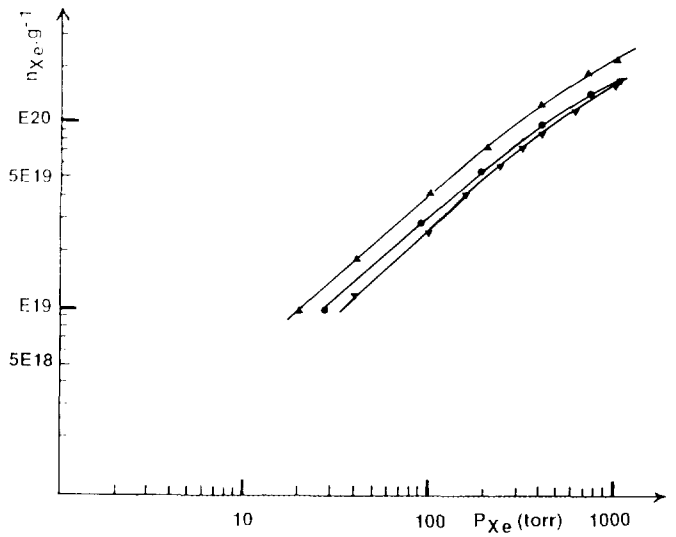

FIG. 3. Xenon adsorption isotherms at 300 K for $M_3PW_{12}O_{40}$: M = NH_4^+, ▲; Cs^+, ●; K^+, ▼.

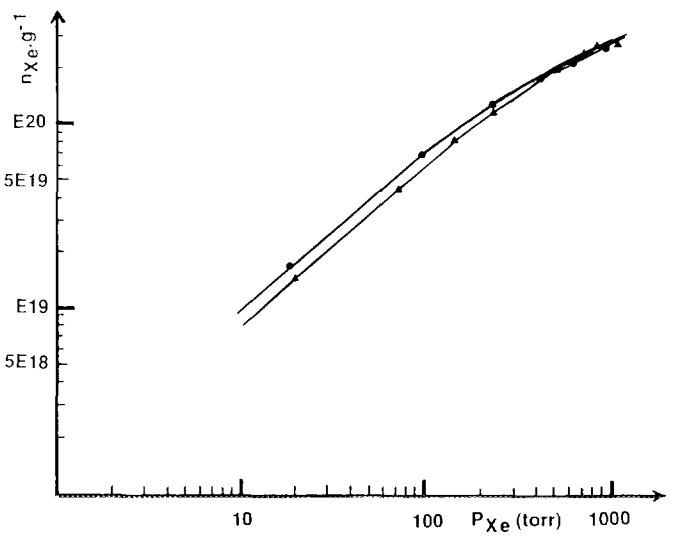

FIG. 5. Xenon adsorption isotherms at 300 K for $M_4SiW_{12}O_{40}$: M = NH_4^+, ▲; Cs^+, ●.

mated errors in the measurements of n_{Xe} and δ are ± 5% and ± 0.5 ppm, respectively.

RESULTS

The Xe adsorption isotherms at 300 K are shown in Figs. 3–5. For a given adsorption equilibrium pressure, with the PW salts, the quantities adsorbed in the range of pressure studied follow the order $NH_4^+ > Cs^+ > K^+$; with PMo salts, $NH_4^+ > Cs^+$; while with SiW salts, the order is $Cs^+ > NH_4^+$. These values appear to be reasonably consistent with those obtained earlier (8, 10) from the adsorption of nitrogen (Table 1).

Despite the small amount of xenon adsorbed, the NMR signal is easily detectable. For all adsorption temperatures and equilibrium pressures, the NMR spectra show only one remarkably narrow signal (40 Hz $< \Delta H <$ 150 Hz) (Fig. 6).

Tests at two additional temperatures (223 and 273 K) show that the chemical shifts are virtually independent of the temperature for NH_4PW, although the $\delta = f(n_{Xe})$ line is displaced downfield by approximately 10 ppm for the cesium salt.

Compression of the NH_4PW and CsPW samples (2T

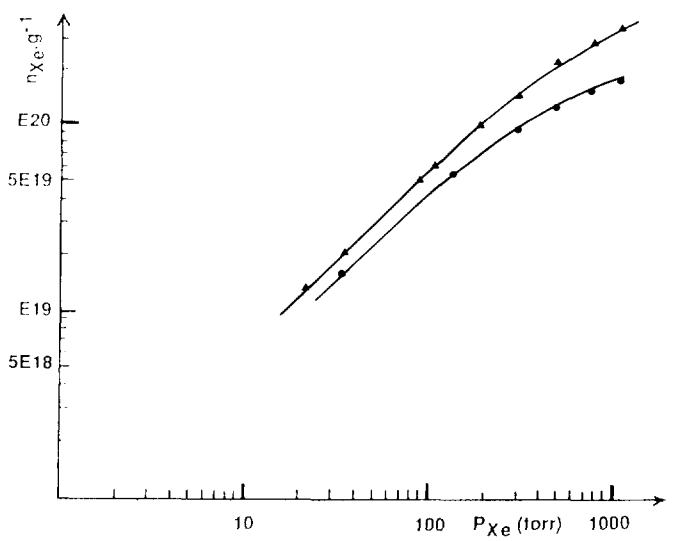

FIG. 4. Xenon adsorption isotherms at 300 K for $M_3PMo_{12}O_{40}$: M = NH_4^+, ▲; Cs^+, ●.

TABLE 1

Sample Characteristics from N_2 Adsorption–Desorption Isotherms at 77 K

Samples	$S_{(BET)}$[a] ($m^2\ g^{-1}$)	V_m[b] ($cm^3\ g^{-1}$)	d(Å)[c]
$(NH_4)_3PW_{12}O_{40}$	128	0.051	20.6
$(K)_3PW_{12}O_{40}$	90	0.033	17.6
$(Cs)_3PW_{12}O_{40}$	163	0.042	27.6
$(NH_4)_3PMo_{12}O_{40}$	193	0.063	26
$(Cs)_3PMo_{12}O_{40}$	146	0.006	28.6
$(NH_4)_4SiW_{12}O_{40}$	117	0.038	19
$(Cs)_4SiW_{12}O_{40}$	153	0.05	21

Note. Estimated errors: S_{BET} (± 2%); V_m (± 5%), d (± 5%).

[a] S_{BET} surface areas are calculated by application of the BET equation to the N_2 adsorption isotherms.

[b] V_m, liquid volume of the micropores.

[c] d, average diameter of the micropores.

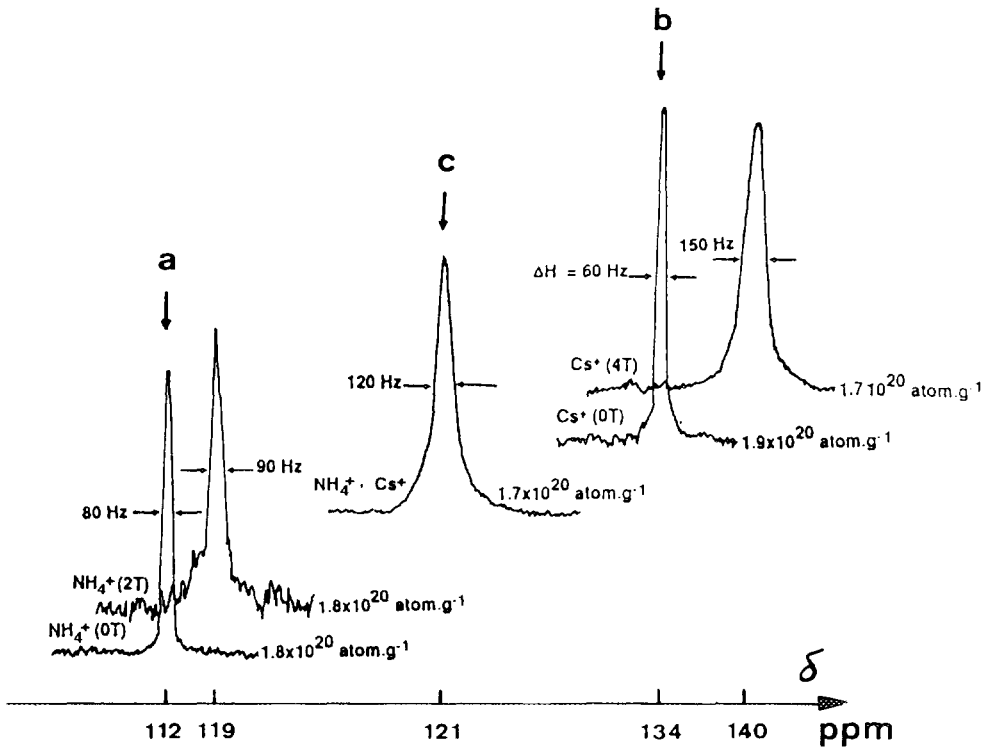

FIG. 6. Shape of Xe^{129} NMR resonance lines of xenon adsorbed on $M_3PW_{12}O_{40}$: (a) $M = NH_4^+$; (b) $M = C_s^+$; (c) mixture 52% (a) + 48% (b) (OT, uncompressed sample; xT, x tonnes cm^{-2} compressed sample).

cm^{-2} and 4T cm^{-2}, respectively) resulted in some broadening of the lines (Fig. 6) and slight downfield displacements (3–6 ppm) of the linear plots, while the slopes remained essentially unchanged (Fig. 7). The xenon adsorption isotherms obtained with the compressed samples were indistinguishable from those of the uncompressed samples.

As found with Y zeolites, the $\delta = f(n_{Xe})$ plots are linear in the range of concentration studied ($n_{Xe} > 2 \times 10^{19}$ atom g^{-1}) regardless of the nature of the samples (Figs. 7–12). With the PW compounds, the slopes of the straight lines are identical for the NH_4^+ and Cs^+ salts, but are significantly higher for the K^+ salt. However, they are in all cases at least five times larger than those observed for a

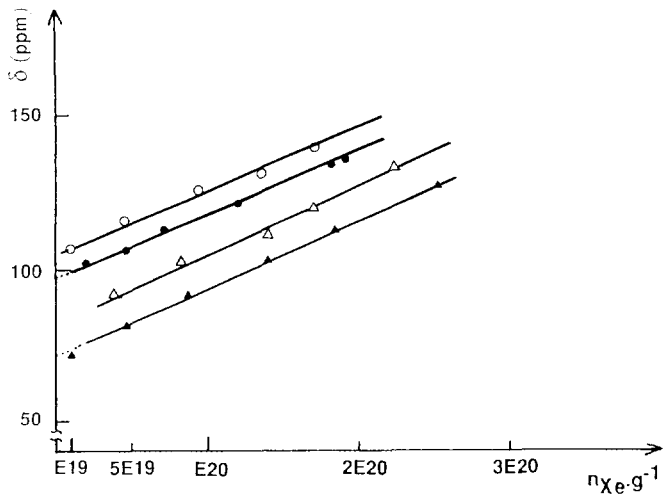

FIG. 7. $\delta = f(n_{Xe})$ curves at 300 K for $M_3PW_{12}O_{40}$: $M = NH_4^+$, ▲; NH_4^+ compressed, △; Cs^+, ●; Cs^+ compressed, ○.

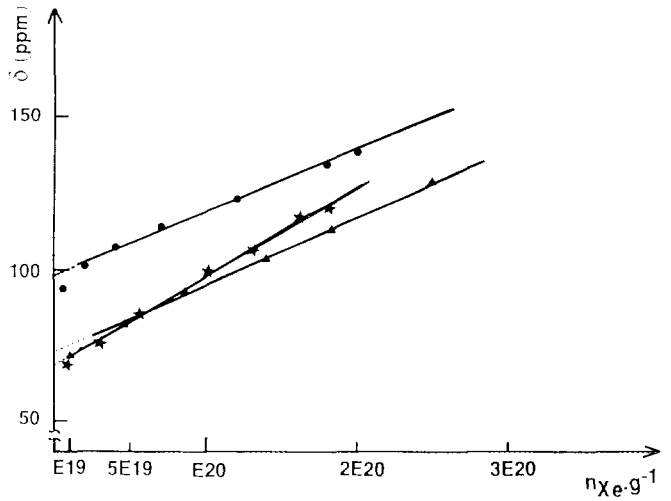

FIG. 8. $\delta = f(n_{Xe})$ curves at 300 K for $M_3PW_{12}O_{40}$: $M = NH_4^+$, ▲; Cs^+, ●; K^+, ★.

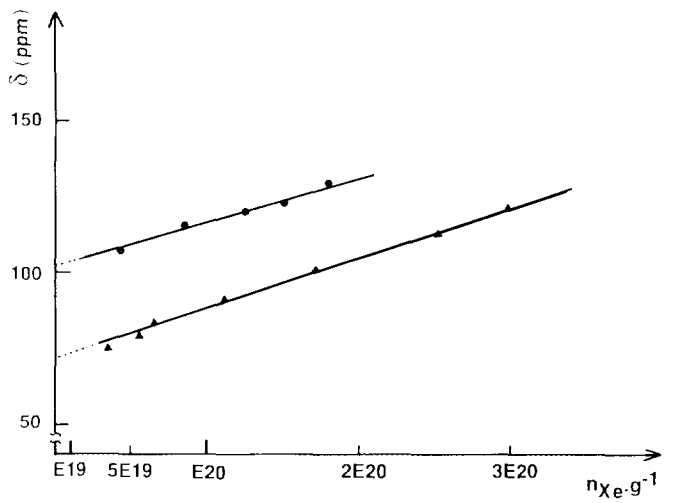

FIG. 9. $\delta = f(n_{Xe})$ curves at 300 K for $M_3PMo_{12}O_{40}$: $M = NH_4^+$, ▲; Cs^+, ●.

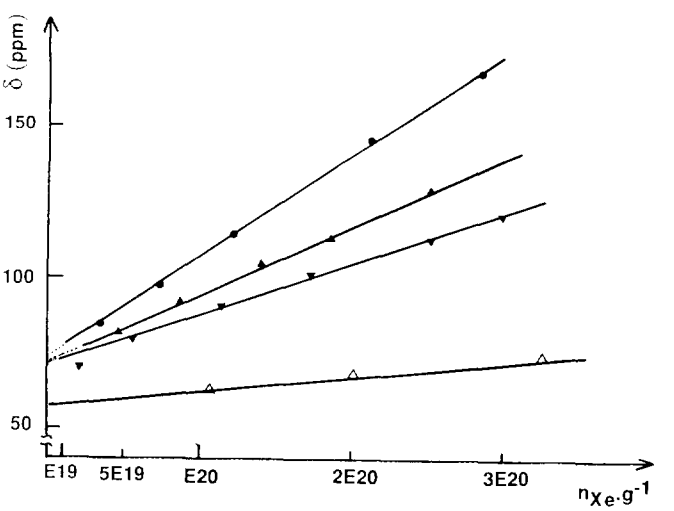

FIG. 11. $\delta = f(n_{Xe})$ curves at 300 K for NH_4^+ salts: $PW_{12}O_{40}$, ▲; $PMo_{12}O_{40}$, ▼; $SiW_{12}O_{40}$, ●; dehydrated NaY zeolite, △.

completely dehydrated NaY zeolite. A similar observation can be made for the PMo compounds. However, with the SiW samples, the slope for the NH_4^+ salt is higher than that of the Cs^+ sample. It should be recalled that this slope is inversely proportional to the free volume of the micropores if the temperature is sufficient to permit the fast exchange between Xe adsorbed on the walls of the lattice and Xe gas inside the micropore.

It is of interest to compare the $\delta = f(n_{Xe})$ plots for the ammonium salts of PW, PMo, and SiW, as well as with that for dehydrated NaY zeolite (Fig. 11). Although the slopes of the straight lines increase in the order SiW > PW > PMo > NaY, the values for the chemical shifts (δ_S) of the MOCC obtained on extrapolation to zero pressure appear to be similar, while that for the zeolite is significantly smaller.

A comparison of the $\delta = f(n_{Xe})$ plots for the cesium salts and the NaY zeolite shows marked differences from the observations for the ammonium salts (Fig. 12). Although the slopes with the cesium salts and the NaY zeolite follow the same order as those with the ammonium salts, the extrapolated values for the MOCC are not coincident.

In a supplementary experiment, a mixture of 52% NH_4PW and 48% CsPW (by weight), which was prepared by grinding in a mortar followed by heating under vacuum at 473 K for 12 h, again showed only one signal over the entire pressure range studied ($0 < P < 1.4 \times 10^5$ Pa).

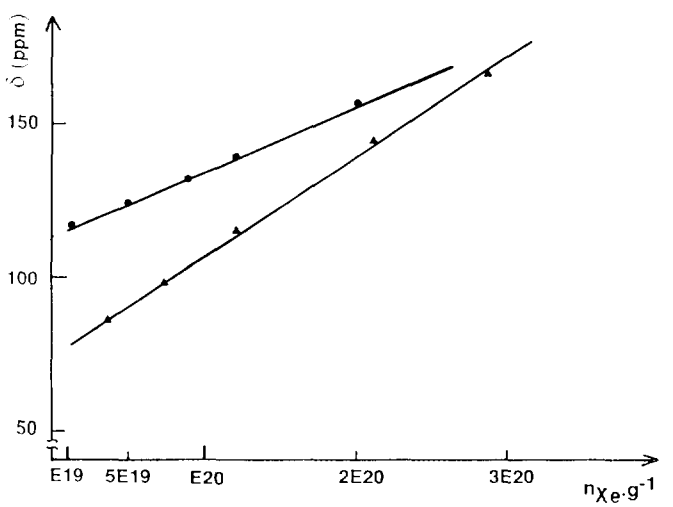

FIG. 10. $\delta = f(n_{Xe})$ curves at 300 K for $M_4SiW_{12}O_{40}$: $M = NH_4^+$, ▲; Cs^+, ●.

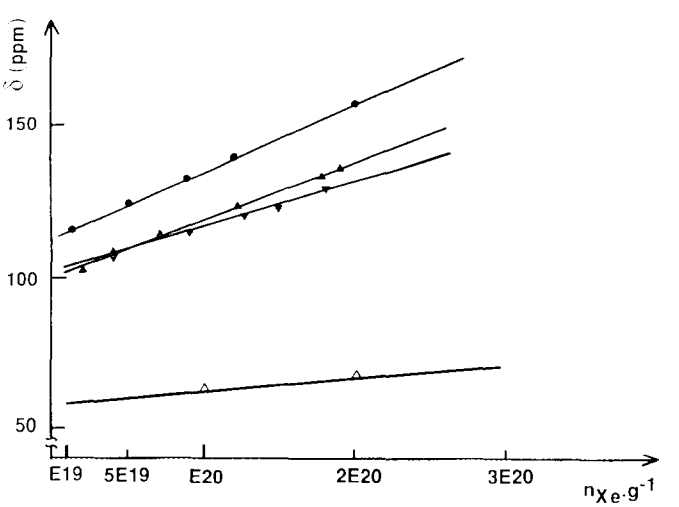

FIG. 12. $\delta = f(n_{Xe})$ curves at 300 K for Cs^+ salts: $PW_{12}O_{40}$, ▲; $PMo_{12}O_{40}$, ▼; $SiW_{12}O_{40}$, ●; dehydrated NaY zeolite, △.

The $\delta = f(n_{Xe})$ plot was linear and fell between and parallel to those obtained for the pure samples. The NMR signal was, however, broadened (Fig. 6), and the width increased when the number of adsorbed xenon atoms decreased.

DISCUSSION

The relative quantities of xenon adsorbed at 300 K at a given adsorption equilibrium pressure on the MOCC salts studied are in semiquantitative agreement with the previous measurements using nitrogen at 77 K, except for that with CsPMo.

The linearity of the $\delta = f(n_{Xe})$ plots is clearly evident from the figures. In the case of no exchange with the gas phase, the linear increase of the chemical shift with the xenon concentration is due to an increase of the Xe–Xe collisions (δ_{Xe-Xe}) in an isotropic environment. In this case, the slope of the $\delta = f(n_{Xe})$ curve is inversely proportional to the void volume. The results obtained from the experiments at variable temperatures and compressions provide evidence in support of this hypothesis.

The narrowness of the signals and the linearity of the $\delta = f(n_{Xe})$ plots strongly suggest that the microporosity is "organized" and as closed as that found in zeolites. For an open porosity and a heterogeneous distribution of pore sizes such as found in alumina or silica gel, for example, the xenon NMR signal would be very difficult to detect at room temperature and the observed lines would be broad. Further, rapid exchange of the adsorbed xenon with the gas phase would result in chemical shifts which are independent of the equilibrium pressure as has been observed by Conner *et al.* (35).

The similarity of the values of δ_S, the chemical shift at zero pressure for the three ammonium salts, is worthy of comment. If it is assumed that the ammonium ion has no electrical effect as in Y zeolites ($\delta_E = 0$) and that the cubic lattice formed by the Keggin anions of the MOCC produces an electric field effect similar to the negatively charged framework of a Y zeolite, the δ_S values obtained (72 ± 2 ppm) for the three samples suggest that the micropore openings are similar and produce from the $\delta_S = f(I)$ curve established by Chen *et al.* (36) a value of 4.6 Å for the mean free path of the xenon.

If the microporous structure is assumed to consist of infinitely long cylindrical cavities, the mean free path is related to the diameter of these cavities, D, by the relation

$$I = D - D_{Xe},$$

where D_{Xe} is the Van der Waals diameter of xenon (4.4 Å). Then, the value of D obtained is 9.0 Å. For spherical cavities, $I = \frac{1}{2}(D - D_{Xe})$ and $D = 13.6$ Å. Although these values are lower than those obtained from the nitrogen adsorption–desorption isotherms (Table 1), it has been shown by Venero and Chiou (37) that, at least for zeolites, nitrogen may be unsuitable for the measurement of pore size distributions as a result of the strong interaction of nitrogen with the charged framework of zeolites due to the large quadrupole moment of nitrogen. Although the structures of zeolites and those of the MOCC are not identical, the hypothesis of Venero and Chiou (37) may be considered as supplying, at least tentatively, a rationalization for the difference between the values obtained from Xe NMR and those from the adsorption–desorption isotherms. Since the lattice parameters for the ammonium salts fall in the range from 11 to 13 Å, the values obtained from Xe NMR appear to be more reasonable than those from the adsorption–desorption isotherms. However, the slopes of the $\delta = f(n_{Xe})$ curves for the three ammonium salts as found in the present work correlate well with the volumes of the micropores obtained previously from analysis of the N_2 adsorption–desorption isotherms (Fig. 13).

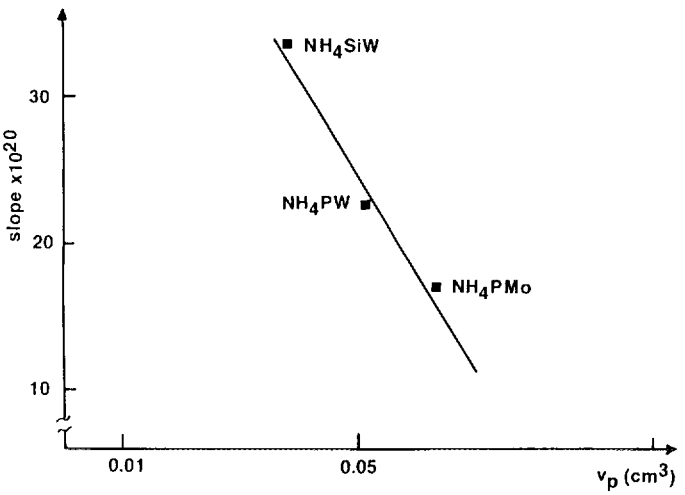

FIG. 13. Correlation between the slope of the $\delta = f(n_{Xe})$ curve and the microporous volume of NH_4^+ MOCC samples.

With the cesium salts the values of δ_S for PMo and PW are 102 and 98 ppm, respectively, approximately 26 ppm higher than those observed for the ammonium salts. The pore diameter values calculated as before are 7.4 and 10.4 Å, for infinite cylinder and closed sphere pore structures, respectively. These values are also low relative to those obtained from the N_2 adsorption–desorption isotherms. A similar shift in the δ_S value was previously observed by Ito and Fraissard (38) for Y zeolites exchanged with large cations (Rb^+, Cs^+, Ba^{2+}). These authors attributed the shift to a large decrease in the mean free path resulting from the restricted diffusion of xenon as a consequence of the high ionic radius of these cations or possibly to the

high polarizability of the cation which perturbs the xenon trajectory, thereby increasing the number of short range collisions. With CsSiW, the value of δ_S (114 ppm) at zero pressure is more downfield shifted (Fig. 10). This difference may result from the 33% larger concentration of cesium ions per anion which is found with SiW in comparison with PW and PMo.

The similarities in the results for the MOCC and Y zeolites suggest that a similar homogeneous and organized porosity exists in both materials. The observations from the experiments at lower temperatures with the MOCC are similar to those found by Chen and Fraissard (39) with ZSM-5 and Y zeolites. For ZSM-5, the $\delta = f(n_{Xe})$ plot is virtually independent of temperature, whereas for Y zeolites a strong dependence on temperature is observed. This difference is tentatively attributed to the density of the structure. More open structures are expected to produce greater temperature dependencies of the chemical shift. The effect of the compression of the MOCC is also similar to that found with zeolites. Compression does not affect the micropore free volume, but by increasing the apparent density of the solid, the residence time of the xenon on the peripheral surface of the crystallites is increased. The chemical shift is then of the form (40)

$$\delta = \left(\frac{1}{1 + (\tau_{inter}/\tau_{intra})}\right) \delta_{intra},$$

where τ_{inter} and τ_{intra} are the xenon residence times between and inside the crystallites, respectively, and δ_{intra} is the chemical shift of xenon inside the micropores. The line broadening upon compression can be attributed to an increase in the heterogeneity of the micropore volume.

The results from the measurements on the NH_4PW/CsPW mixture suggest that either the xenon diffuses very rapidly from a NH_4^+ site to a Cs^+ site or, more probably, the cations have diffused during treatment and are distributed throughout the microporous structure of the sample. The line broadening suggests that the mixture has a more heterogeneous microporous structure than the pure products.

CONCLUSIONS

The results obtained in the present work confirm the presence of microporosity in certain of the monovalent salts of the metal–oxygen cluster compounds. The observed narrow lines provide evidence for the homogeneity and organization of the microporosity. The variations of δ–$f(n_{Xe})$ with the pressure, compression, or temperature are reminiscent of those observed with Y zeolites exchanged with the same cations. The sizes of the pores as obtained from the mean free path of the xenon are lower than those obtained earlier from the nitrogen adsorption–desorption isotherms, but the present values appear to be more consistent with the lattice parameter of the salts. The homogeneity of the microporosity is consistent with the earlier rationalization of the nature and source of the porous structure as based on nitrogen adsorption–desorption isotherms and X-ray diffraction data.

ACKNOWLEDGMENT

Financial support from the Natural Sciences and Engineering Research Council of Canada is gratefully acknowledged.

REFERENCES

1. Occelli, M. L., "Synthesis of Microporous Materials." Van Nostrand–Reinhold, New York, 1992.
2. See, for example, "Selectivity in Catalysis" (M. E. Davis and S. L. Suib, Eds.), ACS Symposium Series, Vol. 517. ACS, Washington, DC, 1993.
3. Lobo, R. F., Pan, M., Chan, I., Li, H.-X., Medrud, R. C., Zones, S. I., Crozier, P. A., and Davis, M. E., *Science* **262,** 1543 (1993).
4. See, for example, "Zeolite Microporous Solids, Synthesis, Structure and Reactivity" (E. G. Derouane, Ed.). Kluwer, Dordrecht, 1992.
5. Scherzer, J., *Catal. Rev.-Sci. Eng.* **31,** 215 (1989).
6. Pope, M. T., "Heteropoly and Isopoly Oxometalates." Springer-Verlag, Berlin, 1983.
7. Brown, C. M., Noe-Spirlet, M. R., Busing, W. R., and Levy, H. A., *Acta Crystallogr. Sect. B* **33,** 1038 (1977).
8. McMonagle, J. B., and Moffat, J. B., *J. Colloid Interface Sci.* **101,** 479 (1984).
9. Highfield, J. G., Hodnett, B. K., McMonagle, J. B., and Moffat, J. B., *in* "Proceedings, 8th International Congress on Catalysis, Berlin, 1984," p. 611. Dechema, Frankfurt-am-Main, 1984.
10. Taylor, D. B., McMonagle, J. B., and Moffat, J. B., *J. Colloid Interface Sci.* **108,** 278 (1985).
11. Moffat, J. B., *Polyhedron* **5,** 261 (1986).
12. Nayak, V. S., and Moffat, J. B., *J. Colloid Interf. Sci.* **120,** 301 (1987).
13. Moffat, J. B., *in* "Preparation of Catalysts IV" (B. Delmon, R. Grange, P. A. Jacobs, and G. Poncelet, Eds.), Studies in Surface Science and Catalysis, Vol. 30. Elsevier, Amsterdam, 1987.
14. Moffat, J. B., McMonagle, J. B., and Taylor, D., *Solid State Ionics* **26,** 101 (1988).
15. McGarvey, G. B., and Moffat, J. B., *J. Colloid Interface Sci.* **125,** 51 (1988).
16. Moffat, J. B., *in* "Studies in Surface Science and Catalysis" (J. Ward, Ed.). Elsevier, Amsterdam, 1988.
17. McMonagle, J. B., Nayak, V. S., Taylor, D., and Moffat, J. B., *in* "Proceedings, 9th International Congress Catalysis, Calgary, 1988" (M. J. Phillips and M. Ternan, Eds.) p. 1804. Chem. Inst. Canada, Ottawa, 1988.
18. Nayak, V. S., and Moffat, J. B., *J. Phys. Chem.* **92,** 7097 (1988).
19. Nayak, V. S., and Moffat, J. B., *J. Phys. Chem.* **92,** 2256 (1988).
20. Nayak, V. S., and Moffat, J. B., *J. Colloid Interface Sci.* **122,** 475 (1988).
21. Nishi, H., Nowinska, K., and Moffat, J. B., *J. Catal.* **116,** 480 (1989).
22. Nishi, H., and Moffat, J. B., *J. Mol. Catal.* **51,** 193 (1989).
23. Moffat, J. B., *J. Mol. Catal.* **52,** 169 (1989).

24. Moffat, J. B., *Chem. Eng. Commun.* **83,** 9 (1989).
25. Moffat, J. B., McGarvey, G. B., McMonagle, J. B., Nayak, V., and Nishi, H., *in* "Guidelines for Mastering the Properties of Molecular Sieves" Barthoment, E. G. Derouane, and W. Hölderich, Eds.), NATO ASI Series D, p. 193. Plenum, New York, 1990.
26. McGarvey, G. B., and Moffat, J. B., *J. Catal.* **128,** 69 (1991).
27. McGarvey, G. B., and Moffat, J. B., *J. Catal.* **130,** 483 (1991).
28. Lapham, D., and Moffat, J. B., *Langmuir* **7,** 2273 (1991).
29. Lapham, D., McGarvey, G. B., and Moffat, J. B., *Stud. Surf. Sci. Catal.* **73,** 261 (1992).
30. McGarvey, G. B., and Moffat, J. B., *in* "Multifunctional Mesoporous Inorganic Solids" (C. A. C. Sequeira, Ed.), p. 451. Kluwer, Dordrecht, 1993.
31. Bonardet, J. L., McGarvey, G. B., Moffat, J. B., and Fraissard, J., *Colloids Surf.* **A72,** 191 (1993).
32. Ito, T., and Fraissard, J., *J. Chem. Phys.* **76,** 5225 (1982).
33. Springuel-Huet, M. A., Demarquay, J., Ito, T., and Fraissard, J., *Stud. Surf. Sci. Catal.* **37,** 183 (1988).
34. Barrie, P. J., and Klinowski, J., *Proc. Nucl. Magn. Reson. Spectrosc.* **24,** 91 (1992).
35. Conner, W. C., Weist, E. L., Ito, T., and Fraissard, J., *J. Phys. Chem.* **93,** 4138 (1989).
36. Chen, Q., Springuel-Huet, M. A., and Fraissard, J., *Stud. Surf. Sci. Catal.* **65,** 219 (1991).
37. Venero, A. F., and Chiou, J. N., *Mater. Res. Soc. Symp. Proc.* **111,** 235 (1988).
38. Ito, T., and Fraissard, J., *J. Chem. Soc. Faraday Trans.* **83,** 451 (1987).
39. Chen, Q., and Fraissard, J., *J. Phys. Chem.* **96,** 1809 (1992).
40. Chen, Q., and Fraissard, J., *J. Phys. Chem.* **96,** 1814 (1992).